Activation of oxygen via accelerating the copper-redox cycle by UV irradiation

Jiamin Hu, Jing Zhang, Lin Yuan and Shuang Lin

ABSTRACT

This study proposes a new method showing that the addition of UV strongly enhanced the oxidation capacity of the Cu(II)/O_2 process, which subsequently produced reactive oxidants using copper as a catalyst via the Fenton-like reactions of *in situ* generated hydrogen peroxide (H_2O_2). Acid orange 7 (AO7) was degraded more than 70% after 70 min at an initial pH of 3.5 in the Cu(II)/O_2/UV process. The mechanism investigation showed that a remarkable amount of Cu(I) and H_2O_2 was produced in the Cu(II)/O_2/UV process, which was due to UV irradiation and activation of oxygen (O_2). The addition of a radical scavenger, tert-butyl alcohol, inhibited AO7 degradation, which verified that hydroxyl radical (·OH) was the primary radical for the degradation of AO7. Superoxide radical ($O_2{\cdot}^-$) was also generated in the Cu(II)/O_2/UV process, indicating that ($O_2{\cdot}^-$) was considered as the intermediate of the production of ·OH. The results showed that the acidic condition was favorable for AO7 degradation, and the degradation of AO7 followed the pseudo-first-order kinetics. The high dosage of Cu(II) enhanced AO7 degradation, but exceeding the optimal dosage of Cu(II) would inhibit AO7 degradation.

Key words | AO7 degradation, copper-redox cycle, hydroxyl radical, oxygen, superoxide radical, UV light irradiation

Jiamin Hu
Jing Zhang (corresponding author)
Lin Yuan
Shuang Lin
College of Architecture & Environment,
Sichuan University,
Chengdu 610065,
China
E-mail: *zjing428@163.com*

INTRODUCTION

Advanced oxidation processes (AOPs), which produce highly reactive and nonselective electrophiles such as ·OH, are dramatic and promising means for nonbiodegradable residual organic contaminants in a wide range of wastewater treatment (Yao *et al.* 2013). The production of ·OH presents the potential to enhance the contaminant degradation rate and the probability of reactions with a wide variety of compounds (Liang & Su 2009). In general, it is usual to use ultrasound, ultraviolet light or transition metals to promote the production of ·OH (Anipsitakis & Dionysiou 2004; Son *et al.* 2012). A number of former studies have found that most transition metals can induce ozone (O_3), H_2O_2 and peroxymonosulfate (PMS) to generate ·OH (Anipsitakis & Dionysiou 2004; Chen *et al.* 2011; Zeng *et al.* 2012; Devi *et al.* 2013; Qin *et al.* 2015). Furthermore, O_2 is also a very common oxidizing agent, which can be induced to generate radicals such as $O_2{\cdot}^-$ and ·OH by transition metals in recent studies (Noradoun & Cheng 2005; Keenan & Sedlak 2008; Liu *et al.* 2011; Zhang *et al.* 2012; Wen *et al.* 2014). For example, zero-valent iron (ZVI) reacted with O_2 to produce ferrous iron at first. Subsequently, ferrous iron reacted with O_2 to generate H_2O_2. Finally, H_2O_2 reacted with ferrous iron via the Fenton reaction to produce ·OH, which then removed the contaminant (Keenan & Sedlak 2008).

Similar to iron, copper (Cu) is a type of essential transition metal. It is well accepted as a kind of remarkable, vital and promising catalyst (Lam *et al.* 2007; Thomas *et al.* 2016). For example, Wen Gang's study showed that

doi: 10.2166/aqua.2017.052

zero-valent copper (ZVC) could react with O_2 like ZVI, which further indicated that Cu(I) could activate O_2 to generate H_2O_2 and radicals (Wen *et al.* 2014). In fact, Cu(II) is the normal valence state that exists in natural water while it has a low potential to activate the oxidants to form radicals (Kolthoff & Woods 1966). On the contrary, Cu(I) is regarded as an excellent activator for oxygen species and a significant scavenger of O_2 (Yuan *et al.* 2012). The main reactions that form a Fenton-like system can be described by Equations (1)–(5) (Pham *et al.* 2012):

$$Cu(I) + O_2 \rightarrow Cu(II) + O_2 \cdot^- \ (k = 1.5\ M^{-1}\ s^{-1}) \quad (1)$$

$$Cu(II) + O_2 \cdot^- \rightarrow Cu(I) + O_2 \ (k = 6.6 \times 10^8\ M^{-1}\ s^{-1}) \quad (2)$$

$$Cu(I) + O_2 \cdot^- \xrightarrow{2H^+} Cu(II) + H_2O_2 \ (k = 2.0 \times 10^9\ M^{-1}\ s^{-1}) \quad (3)$$

$$Cu(I) + H_2O_2 \xrightarrow{-OH^-} Cu(II) + \cdot OH \ (k < 100\ M^{-1}\ s^{-1}) \quad (4)$$

$$Cu(II) + H_2O_2 \xrightarrow{2H^+} Cu(I) + O_2 \cdot^- \ (k = 460\ M^{-1}\ s^{-1}) \quad (5)$$

However, Cu(I) has seldom been investigated as a catalyst in AOPs because it is easily oxidized to Cu(II) in natural waters (Yuan *et al.* 2012). Thus, the redox transformation between Cu(I) and Cu(II) is the most important process to make use of copper in AOPs. Most previous studies have focused principally on the oxygen-dependent oxidation of reducing agents with the purpose of copper-redox cycles (Liu *et al.* 2005; Yuan *et al.* 2013; Zhou *et al.* 2016). For instance, Lee *et al.* (2016) showed that Cu(II) was reduced to Cu(I) by hydroxyl amine (HA), which resulted in the formation of H_2O_2 and the high degradation of benzoic acid (BA). The process indicated that it was quite effective to enhance the ability of oxidation in AOPs via accelerating the copper-redox cycle.

UV is considered as a common type of luminous energy, which is always applied in photo-catalysis and photo-degradation processes (Rosenfeldt *et al.* 2005; Wang *et al.* 2012; Zhong *et al.* 2013; Zou *et al.* 2016; Babel *et al.* 2017; Norzaee *et al.* 2017). For example, the degradation of metolachlor in a water treatment system was a photo-degradation process, which involved both direct UV photolysis as well as the reactions between target compounds and ·OH (Wu *et al.* 2007). The study on the photo-Fenton process by Ahmed *et al.* (2011) verified that UV could reduce Fe(III) to Fe(II) via the photo-reduction process (Wu *et al.* 1999). Based on the above, it is reasonable to consider that UV may be able to reduce Cu(II) to Cu(I), which further activates O_2 to generate H_2O_2 and radicals such as $O_2 \cdot^-$ and ·OH via the transformation between Cu(I) and Cu(II) due to the addition of UV.

In this study, acid orange 7 (AO7) was selected as a target compound for indirectly revealing the production of ·OH. The generation of H_2O_2 and the degradation of AO7 in the Cu(II)/O_2/UV process were investigated. The objects of this study are: (1) to examine whether the oxidation capacity of this process for the degradation of AO7 is promoted due to the addition of UV; (2) to illuminate the mechanism of the generation of H_2O_2 and radicals during this process catalyzed by copper-redox cycle; (3) to investigate the effect of pH, dosage of Cu(II), dosage of AO7, power of UV light and the products of AO7 in the Cu(II)/O_2/UV process.

MATERIALS AND METHODS

Materials

Copper sulfate pentahydrate ($CuSO_4 \cdot 5H_2O$, ≥99.0%) and acid orange 7 (AO7, ≥99.5%) were of analytical purity supplied by Sigma-Aldrich (USA). Hydrogen peroxide (H_2O_2, 30%), tert-butyl alcohol (TBA, ≥99.5%), 1,4-benzoquinone (BQ, ≥99.0%), sodium nitrite ($NaNO_2$, ≥99.0%), carbon tetrachloride (CCl_4, 99.5%), 9,10-diphenylanthracene (DPA, ≥99.0%), sulfuric acid (H_2SO_4, 75%), sodium hydroxide (NaOH, ≥96%), neocuproine hemihydrate (NCP, ≥98%), catalase (≥3,000 units/mg) and N,N-diethyl-1,4-phenylenediammonium (DPD, ≥98%) were of analytical purity and were bought from Sinopharm Chemical Reagent Co., Ltd (China). Methanol, ammonium acetate and acetonitrile were chromatographically pure and were bought from Sinopharm Chemical Reagent Co., Ltd (China). Pure oxygen (O_2, ≥99.2%) and pure nitrogen (N_2, ≥99.9%) were stored in a special high-pressure gas cylinder.

Procedures

Most experiments were carried out at ambient temperature (20 ± 1 °C) in a 1,000 mL cylindrical glass reactor using a quartz tube with a diameter of 35 mm and a 15 W low pressure (LP) UV lamp peaking at 254 nm, while there were also a few experiments with 8, 25, 40 and 80 W LP lamps. The reactor was surrounded by condensated water with the purpose of keeping the temperature of the sample constant. The UV lamp was placed in a quartz tube to stop the UV lamp from short circuiting. Cu(II) ($CuSO_4{\cdot}5H_2O$) and AO7 at the desired concentrations were spiked into 1,000 mL pure water. The initial pH was adjusted by H_2SO_4 or NaOH. Each run was started by UV light emission. BQ, TBA and DPA were regarded as scavengers of $O_2{\cdot}^-$, ·OH and singlet oxygen ($^1O_2$) in the quenching experiments, respectively, which was introduced in excess at once after UV light emission. Samples detected by high performance liquid chromatography (HPLC) and liquid chromatography/mass spectrometry (LC/MS) were quenched by $NaNO_2$ after being withdrawn.

Analysis

AO7 in all experiments (except for the experiments of BQ addition) and the absorbance of DPA were measured by a UV-vis spectrometer (MAPADA, UV-1800) at 484 and 374 nm using a 1 cm quartz cuvette, respectively. The absorbance of DPA at 374 nm could be used to investigate the generation of $^1O_2$ (Jun *et al.* 1992; Zhao & Zhang 2005). The concentration of AO7 in the presence of BQ was detected by HPLC (Waters e2695, USA) equipped with a reverse-phase C18 column (4.6 × 150 mm) in order to avoid interference of different peaks at 484 nm (Qi *et al.* 2016). The mobile phase was methanol and 20 mM ammonium acetate (85:15, v/v) at 1 mL·min^{-1}. Detection was performed via a 2,489 λ UV absorbance detector set at 484 nm. The injection volume was 50 μL and the column temperature was 35 °C.

The products of AO7 were determined by LC/MS (Finnigan TSQ Quantum Ultra, USA) equipped with a Thermo Scientific Hypersil Gold C18 column (2.1 × 200 mm × 1.9 μm) via electrospray ionization (ESI) interface. The mobile phase was 10 mM ammonium acetate (A) and acetonitrile (B). A linear gradient elution was performed beginning with 98% A and 2% B at 0.5 mL·min^{-1} at 5 min, then 98% A and 2% B at 1.2 mL·min^{-1} at 7 min, and finally 5% A and 95% B at 1.2 mL·min^{-1} at 30 min. The analysis conditions were as follows: column temperature: 30 °C; injection volume: 10 μL; spectra were obtained in a scan range: 100–500 m/z; determination wavelength: 254 nm.

Total organic carbon (TOC) was measured by a TOC analyzer (Liqui II, Germany). The concentration of H_2O_2 was measured by a photometric method (Bader *et al.* 1988). The concentration of Cu(I) was spectrophotometrically determined by the neocuproine method (American Public Health Association *et al.* 2005). Moreover, pH level was measured by a pH meter (pHs-25), and changed less than ±0.1. A dissolved oxygen (DO) meter (JPB-607A) was used to measure the concentration of DO. Each experiment was carried out three times and the standard deviation gained was no more than 4.0%.

RESULTS AND DISCUSSION

Comparison of different processes

Figure 1 shows the degradation of AO7 in the O_2, Cu(II), Cu(II)/O_2, O_2/UV and Cu(II)/O_2/UV processes, respectively. As shown in the graph, neither Cu(II) nor O_2 alone changed the concentration of AO7. The Cu(II)/O_2 process did not degrade AO7 either, suggesting that O_2 could hardly be activated by Cu(II). In addition, AO7 was only degraded 40% by the O_2/UV process, which conformed with the fact that UV could photodegrade AO7 directly and activate O_2 to result in the generation of H_2O_2 (Wang *et al.* 2014). The combination of Cu(II) with UV under O_2 conditions (Cu(II)/O_2/UV) degraded AO7 by more than 70% in 70 min. It is obvious that the addition of UV light irradiation strongly enhanced oxidation in the Cu(II)/O_2/UV process.

Pathway of the generation of H_2O_2 and radicals

Identification of radicals

According to Equations (1)–(5), O_2 was induced to generate $O_2{\cdot}^-$ by Cu(I) directly at first, then Cu(I) reacted with $O_2{\cdot}^-$ to produce H_2O_2, and Cu(I) activated H_2O_2 to generate

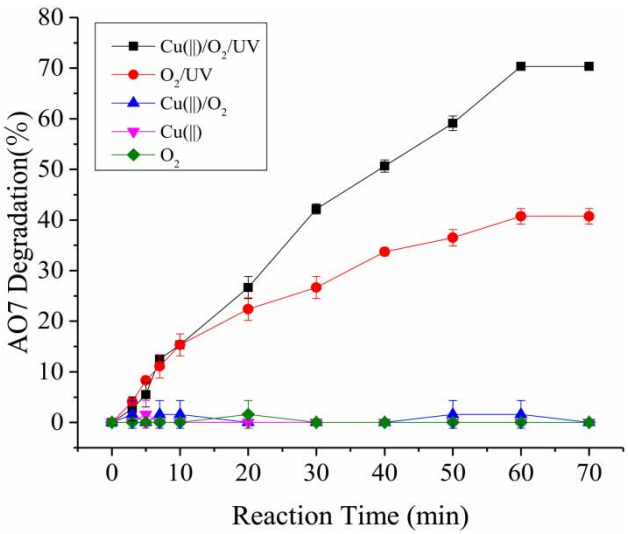

Figure 1 | Time-dependent degradation of AO7 by O_2, Cu(II), Cu(II)/O_2, UV/O_2 and Cu(II)/O_2/UV processes. Experimental conditions: $[Cu(II)]_0 = 10\ \mu M$, $[AO7]_0 = 1.5\ \mu M$, power of UV light = 15 W, O_2 flow rate = 0.5 L·min^{-1}, pH = 3.5 ± 0.1, 20 °C, reaction time = 70 min.

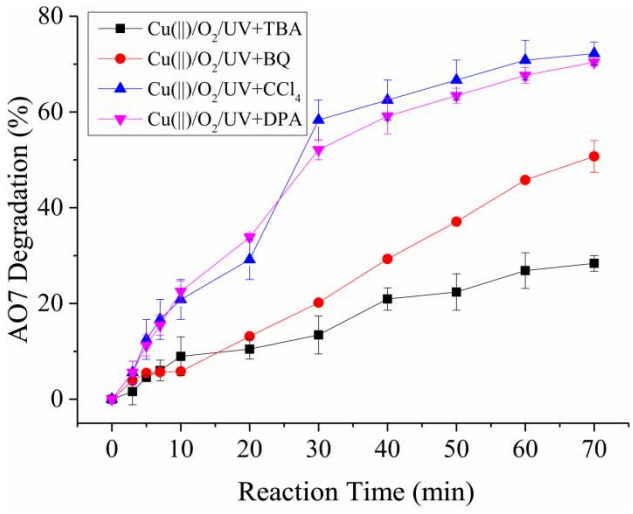

Figure 2 | Effect of the addition of different radical scavengers on AO7 degradation in the Cu(II)/O_2/UV process. Experimental conditions: $[Cu(II)]_0 = 10\ \mu M$, $[AO7]_0 = 1.5\ \mu M$, $[TBA]_0 = 25$ mM, $[BQ]_0 = 0.15$ mM, $[DPA]_0 = 2.0\ \mu M$, power of UV light = 15 W, O_2 flow rate = 0.5 L·min^{-1}, pH = 3.5 ± 0.1, 20 °C, reaction time = 70 min.

·OH finally. Thus, $O_2{\cdot}^-$ and ·OH may be two main radicals in the Cu(II)/O_2/UV process. In order to identify different species of radicals in the Cu(II)/O_2/UV process, TBA and BQ, which have a high reaction rate with ·OH ($k = 5.0 \times 10^8\ M^{-1}\ s^{-1}$) and $O_2{\cdot}^-$ ($k = 0.9$–$1.0 \times 10^9\ M^{-1}\ s^{-1}$), were introduced (Ma & Graham 2000; Qi *et al.* 2016). As shown in Figure 2, the degradation of AO7 in the Cu(II)/O_2/UV process with TBA was strongly decreased to 28% in 70 min. The reason for this phenomenon may be that TBA could inhibit the production of ·OH, but a part of AO7 could also be degraded via photo-degradation by UV. Besides, AO7 degradation rate in the Cu(II)/O_2/UV + BQ process was decreased to 51% during the same reaction time, which had a weaker effect on AO7 degradation compared with the former process. The results indicated that ·OH was the primary radical for AO7 degradation in the Cu(II)/O_2/UV process, and $O_2{\cdot}^-$, which could be considered as a intermediate of the production of ·OH (Equations (1)–(5)), was also generated in this AOPs.

Singlet oxygen, another common free radical, could be generated via photosensitization or the reaction between $O_2{\cdot}^-$ and ·OH, as shown in the following Equation (6) (Bokare & Choi 2015; Li *et al.* 2015; Qi *et al.* 2016). In order to investigate whether $^1O_2$ was generated in the Cu(II)/O_2/UV process, DPA, a scavenger of $^1O_2$ ($k = 1.3 \times 10^6\ M^{-1}\ s^{-1}$), was introduced (Wasserman *et al.* 1972). DPA can only dissolve in organic solvents like CCl_4, so the experiment of the addition of CCl_4 was included to exclude the interference of CCl_4. As shown in Figure 2, the Cu(II)/O_2/UV+ CCl_4 process had no obvious effect on the AO7 degradation compared with the Cu(II)/O_2/UV process in Figure 1. During 70 min, the AO7 degradation rate in the Cu(II)/O_2/UV + DPA process was only decreased less than 2%, indicating that a small amount of $^1O_2$ may be generated in the Cu(II)/O_2/UV process. To further investigate how $^1O_2$ was generated, the changes of the absorbance of DPA at 374 nm were detected in the Cu(II)/O_2/UV process with AO7 and without AO7. As shown in Figure 3, the changes of the absorbance of DPA were tiny and similar under these two conditions, which demonstrated that $^1O_2$ was generated via the reaction between $O_2{\cdot}^-$ and ·OH instead of photosensitization. Both the results in Figures 2 and 3 indicated that $^1O_2$ was not a primary radical in the Cu(II)/O_2/UV process:

$$O_2{\cdot}^- + {\cdot}OH \rightarrow {}^1O_2 + OH^- \quad (6)$$

The generation of H_2O_2

The generation of H_2O_2 was believed to be the precursor of ·OH in the Cu(II)/O_2/UV process. To investigate the

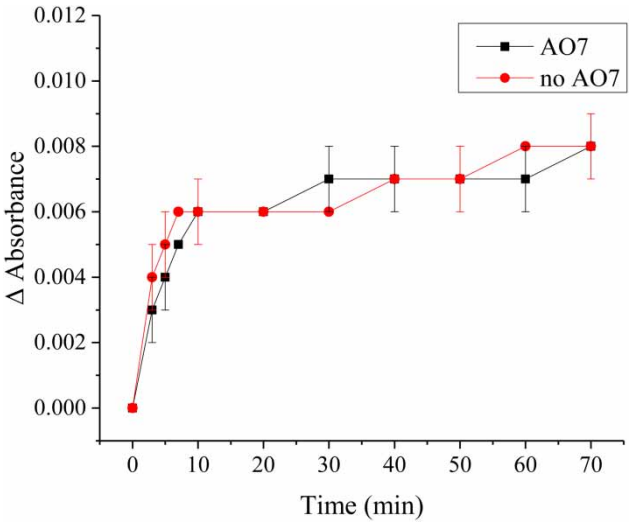

Figure 3 | Change of the absorbance of DPA in the Cu(II)/O_2/UV with AO7 and without AO7 processes. Experimental conditions: $[Cu(II)]_0 = 10$ μM, $[AO7]_0 = 1.5$ μM, $[DPA]_0 = 2.0$ μM, power of UV light = 15 W, O_2 flow rate = 0.5 L·min^{-1}, pH = 3.5 ± 0.1, 20 °C, reaction time = 70 min.

generation of H_2O_2, the concentrations of H_2O_2 were examined in the O_2/UV, Cu(II)/O_2, Cu(II)/O_2/UV and Cu(II)/N_2/UV processes without the addition of AO7. As shown in Figure 4, the Cu(II)/O_2/UV process produced a higher concentration of H_2O_2 than the O_2/UV process; the Cu(II)/O_2 process did not produce H_2O_2. Moreover, the concentration of H_2O_2 in the Cu(II)/N_2/UV process was lower than that in the Cu(II)/O_2/UV process, which may be related to the concentrations of DO. Based on the sequence of Equations (1)–(5), the generation of H_2O_2 occurred first and then H_2O_2 began to be consumed later, which was consistent with the results in the Cu(II)/N_2/UV and Cu(II)/O_2/UV processes as shown in Figure 4. In addition, the concentration of H_2O_2 was low, which may be because UV could decompose a part of H_2O_2 (Xu *et al.* 2017).

The role of O_2 in the Cu(II)/O_2/UV process

Oxygen is likely to be the precursor of H_2O_2 based on the above illumination. To investigate the effect of oxygen, the oxidative degradation of AO7 by the Cu(II)/UV process was examined at pH 3.5 under different aeration conditions. As shown in Figure 5, the Cu(II)/UV process with no aeration (open to the atmosphere) showed a slightly higher AO7 degradation rate than that with N_2 aeration (Cu(II)/N_2/UV). In contrast, the degradation of AO7 in the Cu(II)/O_2/UV process was much higher than in those two processes, which indicated that the higher concentration of DO in aqueous solution had a stronger effect on the oxidative degradation of AO7 due to the higher concentration

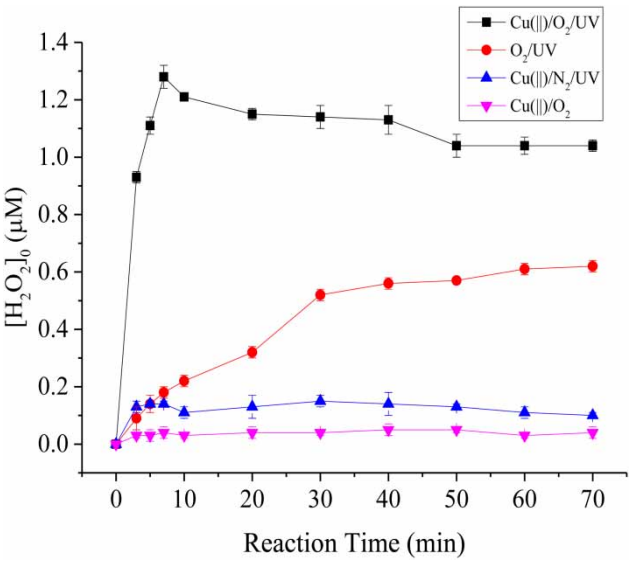

Figure 4 | The concentrations of H_2O_2 in the Cu(II)/O_2, O_2/UV, Cu(II)/O_2/UV and Cu(II)/N_2/UV processes. Experimental conditions: $[Cu(II)]_0 = 50$ μM, power of UV light = 15 W, O_2 flow rate = 0.5 L·min^{-1}, pH = 3.5 ± 0.1, 20 °C, reaction time = 70 min.

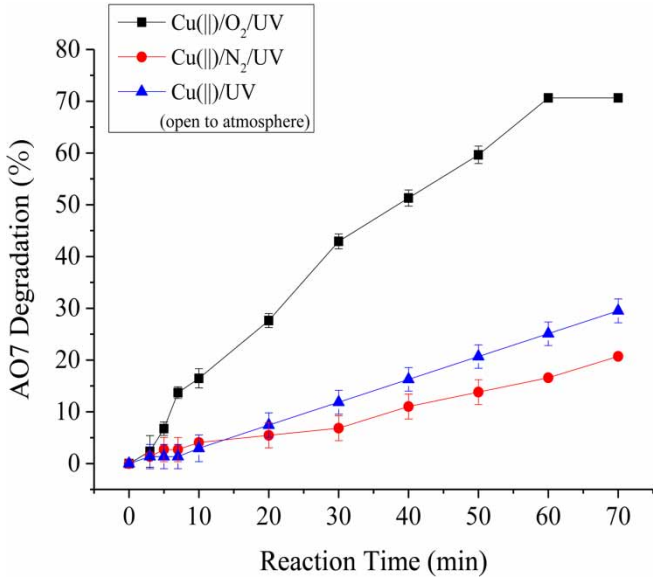

Figure 5 | The role of O_2 in the Cu(II)/O_2/UV process. Experimental conditions: $[Cu(II)]_0 = 10$ μM, $[AO7]_0 = 1.5$ μM, power of UV light = 15 W, O_2 flow rate = 0.5 L·min^{-1}, N_2 flow rate = 0.5 L·min^{-1}, pH = 3.5 ± 0.1, 20 °C, reaction time = 70 min.

of H_2O_2 as shown in Figure 4. Thus, the Cu(II)/UV process without oxygen is not able to produce H_2O_2, which explains why the Cu(II)/N_2/UV process can only degrade a small amount of AO7.

The transformation between Cu(I) and Cu(II)

Based on the above description, Cu(I) could activate O_2 to promote the generation of H_2O_2, and meanwhile Cu(I) was oxidized to Cu(II). It has been proposed that the decomposition of H_2O_2 catalyzed by the copper-redox could produce ·OH. The presence of Cu(I) may be a key factor to affect the oxidation capacity towards the Cu(II)/O_2/UV process, which is associated with Cu(II) reduction in the presence of UV. To examine the production of Cu(I), the concentrations of Cu(I) were monitored in the Cu(II)/O_2, Cu(II)/O_2/UV and Cu(II)/N_2/UV processes without the addition of AO7, respectively. As shown in Figure 6, the concentration of Cu(I) in the Cu(II)/O_2/UV process was lower than that in the Cu(II)/N_2/UV process; the combination of Cu(II) and O_2 without UV did not produce Cu(I). The comparison of the Cu(II)/O_2 and Cu(II)/O_2/UV processes indicated that UV could reduce Cu(II) to Cu(I). In addition, the comparison of the Cu(II)/O_2/UV and Cu(II)/N_2/UV processes may manifest that a part of Cu(I) was oxidized to Cu(II) by $O_2{\cdot}^-$ as described in Equation (3).

To conclude, the addition of UV could effectively promote the transformation between Cu(I) and Cu(II), which further enhanced the efficiency of activating O_2 to generate H_2O_2 and ·OH. This process could be summarized as the simple Equations (7)–(9), showing that the copper-redox cycle catalyzed the reactions between O_2 and UV.

$$\mathrm{Cu(II)} \xrightarrow{\mathrm{hv}} \mathrm{Cu(I)} \tag{7}$$

$$2\mathrm{Cu(I)} + \mathrm{O_2} \xrightarrow{2\mathrm{H^+}} 2\mathrm{Cu(II)} + \mathrm{H_2O_2} \tag{8}$$

$$\mathrm{Cu(I)} + \mathrm{H_2O_2} \xrightarrow{-\mathrm{OH^-}} \mathrm{Cu(II)} + \cdot\mathrm{OH} \tag{9}$$

Effect of pH

The effect of pH on the degradation of AO7 ranging from 2.95 to 6.09 was studied in order to further investigate the mechanism of the Cu(II)/O_2/UV process. As shown in Figure 7, the degradation of AO7 was decreased with an

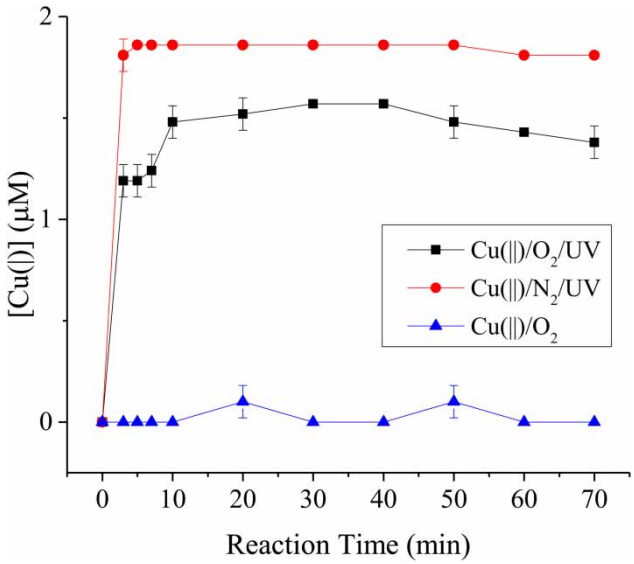

Figure 6 | The concentrations of Cu(I) in the Cu(II)/O_2, Cu(II)/O_2/UV and Cu(II)/N_2/UV processes. Experimental conditions: $[Cu(II)]_0 = 50$ μM, power of UV light = 15 W, O_2 flow rate = 0.5 L·min^{-1}, N_2 flow rate = 0.5 L·min^{-1}, pH = 3.5 ± 0.1, 20 °C, reaction time = 70 min.

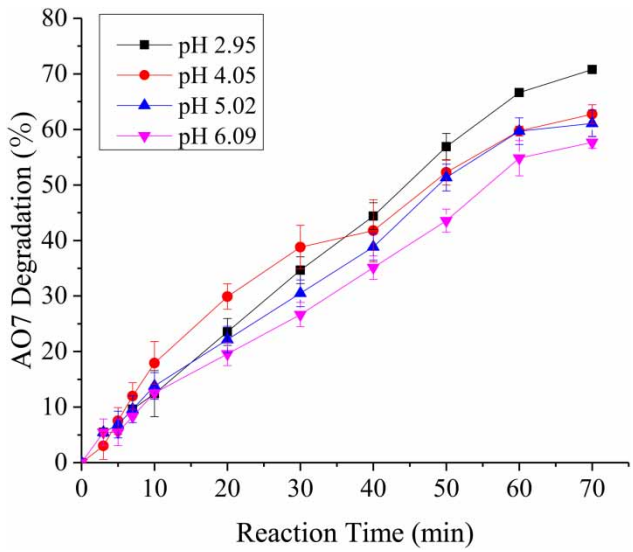

Figure 7 | Effect of pH on the degradation of AO7 in the Cu(II)/O_2/UV process. Experimental conditions: $[Cu(II)]_0 = 10$ μM, $[AO7]_0 = 1.5$ μM, power of UV light = 15 W, O_2 flow rate = 0.5 L·min^{-1}, pH = 2.95, 4.05, 5.02 and 6.09, 20 °C, reaction time = 70 min.

increase of pH level. For example, at pH 2.95, over 70% of AO7 was removed in 70 min. On the contrary, AO7 was degraded 60% at initial pH ranging from 4.05 to 5.02 and 55% at initial pH 6.09. These results confirmed that the acidic condition was favorable for AO7 degradation. One possible reason may be that the solubility product (k_{sp}) of $Cu(OH)_2$ is 1.6×10^{-19} (Kang *et al.* 2014), and the maximum concentrations of Cu(II) in aqueous solution at pH 3, 4, 5 and 6 are 1.6×10^{3}, 1.6×10^{1}, 1.6×10^{-1} and 1.6×10^{-3} mol L^{-1}, respectively. High pH level can lead to the precipitation of copper, which reduces the production of Cu(I). Based on the description above, the generation of H_2O_2 and ·OH was also decreased in this condition, which further resulted in the inhibition of AO7 degradation.

Effect of dosage of Cu(II)

Based on the description above, copper serves as a catalyst, and the presence of Cu(I) is one of the key factors affecting the oxidation capacity towards the Cu(II)/O_2/UV process. Thus, to investigate the effect of Cu(II) on AO7 degradation, different dosages of Cu(II) were examined at pH 3.5. As shown in Figure 8, the higher concentration of Cu(II) could enhance the degradation of AO7. It may be because an increased dosage of Cu(II) could facilitate the production of Cu(I), which could accelerate the decomposition of H_2O_2 into ·OH via Equations (3) and (4). The optimal dosage of Cu(II) was 50 μM. Exceeding the optimal concentration of Cu(II) led to a slight reduction of AO7 degradation, which may be because Cu(I) can react with ·OH to inhibit the degradation of AO7 following Equation (10) (Buxton *et al.* 1988):

$$Cu(I) + \cdot OH \rightarrow Cu(II) + OH^- \quad (10)$$

Effect of power of UV light

The effect of power of UV light on AO7 degradation was examined with 8, 25, 40 and 80 W UV lights in the Cu(II)/O_2/UV process. As shown in Figure 9, 40 and 80 W UV lights degraded AO7 entirely within 10 min. However, AO7 degradation rate reached 60% with 8 W UV light and 90% with 25 W UV light within 70 min. Therefore, the degradation of AO7 was strongly increased with an increase of the power of UV light. This may be because the high power of UV light can accelerate the production of Cu(I), which enhances the generation of H_2O_2 and further results in the generation of ·OH.

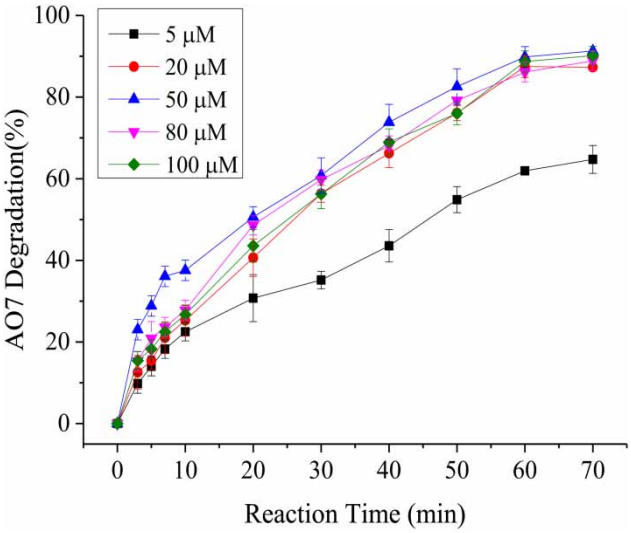

Figure 8 | Effect of dosage of Cu(II) on the degradation of AO7 in the Cu(II)/O_2/UV process. Experimental conditions: $[Cu(II)]_0 = 5$, 20, 50, 80 and 100 μM, $[AO7]_0 = 1.5$ μM, power of UV light = 15 W, O_2 flow rate = 0.5 L·min^{-1}, pH = 3.5 ± 0.1, 20 °C, reaction time = 70 min.

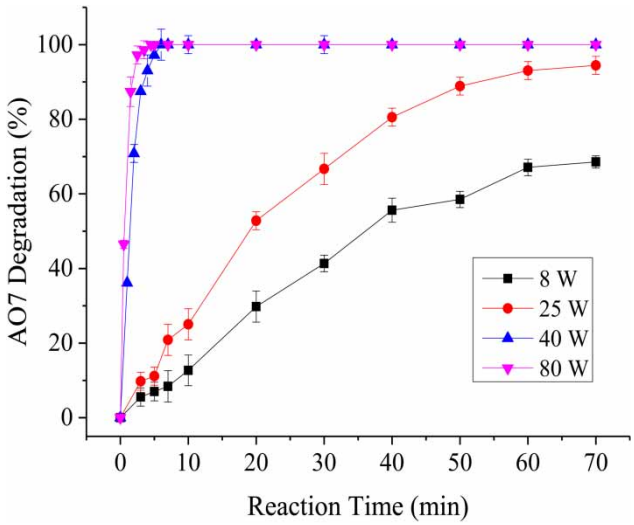

Figure 9 | Effect of power of UV light on the degradation of AO7 in the Cu(II)/O_2/UV process. Experimental conditions: $[Cu(II)]_0 = 10$ μM, $[AO7]_0 = 1.5$ μM, O_2 flow rate = 0.5 L·min^{-1}, power of UV light = 8, 25, 40 and 80 W, pH = 3.5 ± 0.1, 20 °C, reaction time = 70 min.

Effect of dosage of AO7

The effect of dosage of AO7 on the degradation of AO7 ranging from 1 to 7.5 μM was studied. As shown in Figure 10(a), an increased dosage of AO7 inhibited the degradation of AO7, which conformed with the general rule. In principle, the target compound degradation should be describable with a pseudo-first order rate constant (Waldemer *et al.* 2007). Previous studies confirmed that the kinetics of the degradation of AO7 in the UV/H_2O_2 process is the pseudo-first order kinetics model (Behnajady *et al.* 2004). The mechanism in the Cu(II)/O_2/UV process is similar to that in the UV/H_2O_2 process, which shows that the Cu(II)/O_2/UV process may accord with the pseudo-first order kinetics model as well.

To investigate the kinetics of AO7 degradation in the Cu(II)/O_2/UV process, different dosages of AO7 were studied. As shown in Figure 10(b), this result is in good agreement with the pseudo-first order kinetics model. The reaction rate equation of AO7 degradation can be described as Equation (11). Rate constants (k) and R^2 ($R^2 > 0.992$) of different dosages of AO7 are summarized in Table 1. The reaction rate of AO7 degradation depends on the initial concentration of AO7. Decreased k was observed with the increasing concentration of AO7, indicating that the lower reaction rate was observed when the higher dosage of AO7 was added to the samples. This could explain the observation which is shown in Figure 10(a):

$$-\ln\frac{[\mathrm{AO7}]_t}{[\mathrm{AO7}]_0} = kt \tag{11}$$

Products of AO7

To investigate the efficiency of the Cu(II)/O_2/UV process and whether AO7 was oxidized completely, TOC degradation in this process was detected. As shown in Figure 11, TOC was removed over 54% during 70 min, and it had an increasing trend. The result indicated that AO7 was nearly decomposed to CO_2, not just decolorized.

In order to determine the degradation process of AO7, the UV full scan was examined in the Cu(II)/O_2/UV process. The absorption peaks of 230 and 311 nm in the ultraviolet region are the conjugated system of benzene ring and naphthalene ring because of π-π* transition (Bauer *et al.* 2001). In addition, the absorption peaks of 485 and 430 nm in the visible light region are two isomerides of the structures of hydrazone and monoazo because of n-π* transition (Wu *et al.* 2000). As shown in Figure 12, the major peak between 400 and 550 nm, $\lambda_{max} = 484$ nm, accounts for the orange color and can be attributed to the azo linkage, which was observed to show decreasing absorbance from 0 to 70 min. During the degradation process of AO7, hydrazone and monoazo may decompose into

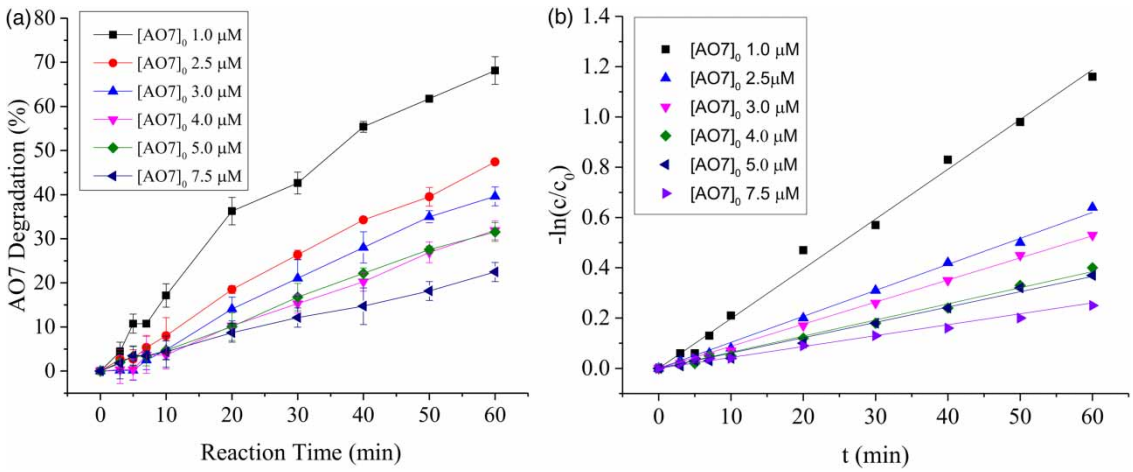

Figure 10 | (a) Effect of dosage of AO7 on AO7 degradation in the Cu(II)/O_2/UV process, and (b) linear fit of rate constants from kinetic models for the degradation of AO7 in the Cu(II)/O_2/UV process. Experimental conditions: $[Cu(II)]_0 = 10$ μM, $[AO7]_0 = 1.0$, 2.5, 3.0, 4.0, 5.0 and 7.5 μM, O_2 flow rate = 0.5 L·min^{-1}, power of UV light = 15 W, pH = 3.5 ± 0.1, 20 °C, reaction time = 60 min.

Table 1 | Pseudo-first order rate constants for the degradation of AO7 by Cu(II)/O_2/UV process under the conditions of different dosages of AO7

[AO7], μM	1	2.5	3	4	5	7.5
k, min^{-1}	0.019	0.010	0.008	0.006	0.006	0.004
R^2	0.994	0.995	0.996	0.993	0.992	0.992

Experimental conditions: $[Cu(II)]_0 = 10$ μM, $[AO7]_0 = 1.0$, 2.5, 3.0, 4.0, 5.0 and 7.5 μM, power of UV light = 15 W, O_2 flow rate = 0.5 L·min^{-1}, pH = 3.5 ± 0.1, 20 °C, reaction time = 60 min.

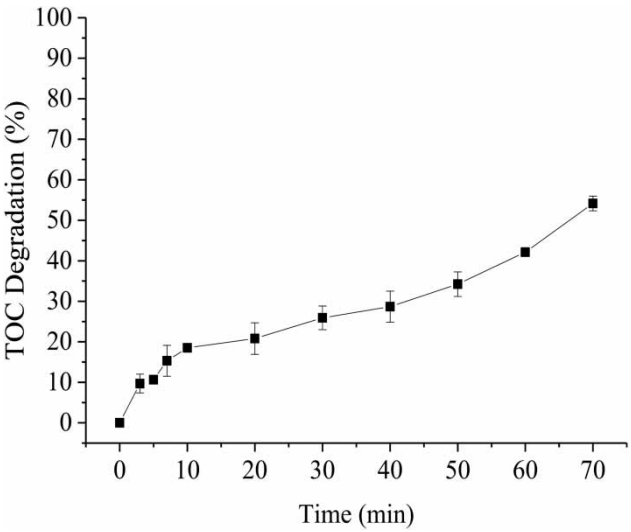

Figure 11 | TOC degradation in the Cu(II)/O_2/UV process. Experimental conditions: $[Cu(II)]_0 = 10$ μM, $[AO7]_0 = 1.5$ μM, power of UV light = 15 W, O_2 flow rate = 0.5 L·min^{-1}, pH = 3.5 ± 0.1, 20 °C, reaction time = 70 min.

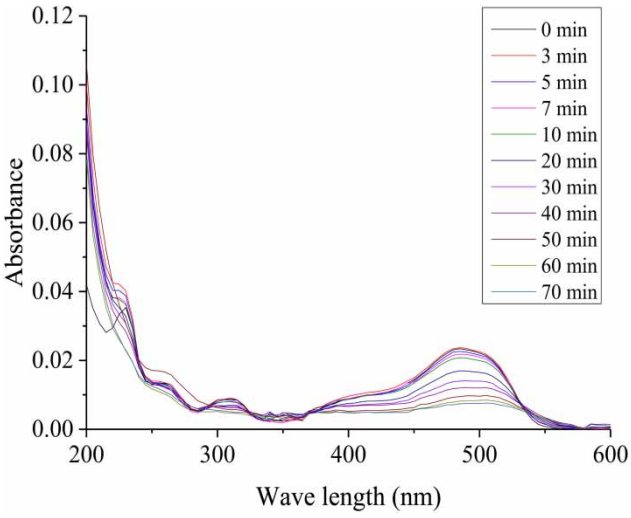

Figure 12 | The UV full scan in the Cu(II)/O_2/UV process. Experimental conditions: $[Cu(II)]_0 = 10$ μM, $[AO7]_0 = 1.5$ μM, power of UV light = 15 W, O_2 flow rate = 0.5 L·min^{-1}, pH = 3.5 ± 0.1, 20 °C, reaction time = 70 min.

benzene rings and naphthalene rings. Therefore, the products of AO7 degradation were determined by LC/MS to further investigate how AO7 was removed, and the intermediates of AO7 are listed in Table 2. As shown in Table 2, p-benzoquinone, 2-(3-hydroxypropyl) phenol, 3,4-dihydronaphthalene-1(2H) and 3-(2-aminophenyl) propanoic acid were detected at 5 min in the Cu(II)/O_2/UV process. According to the results of LC/MS, the degradation process of AO7 could be presented as shown in Figure 13. It is obvious that the azo linkage fractured first, and then may be decomposed to 1-amino-2-naphthol and p-aminobenzene sulfonic acid (Qi *et al.* 2016). Subsequently, these two parts were further decomposed to small molecules like p-benzoquinone via the ring-opening reaction, oxidation reaction, substitution reaction and addition reaction. Finally, these small molecules were further oxidized to CO_2 and H_2O, which was in good agreement with the result of TOC as shown in Figure 11.

CONCLUSIONS

In this study, the degradation of AO7 using ·OH generated via activation with Cu(II) and O_2 by UV irradiation was investigated. The Cu(II)/O_2/UV process showed the best performance via the comparison of different processes. It clearly demonstrated that the Cu(II)/O_2/UV process produces ·OH via the Fenton-like reactions of *in situ* generated Cu(I) and H_2O_2. AO7 degradation can be described as the following process: Above all, Cu(II) is reduced to Cu(I) by UV light irradiation. Subsequently, Cu(I) activates O_2 to generate $O_2{\cdot}^-$, and then H_2O_2 is generated via the reaction between $O_2{\cdot}^-$ and Cu(I). Finally, the reaction between Cu(I) and H_2O_2 produces ·OH, which further results in the degradation of AO7 and the regeneration of Cu(II). In fact, copper can be considered as a catalyst during this process and enhances the oxidation capacity of the O_2/UV process for AO7 degradation. Oxygen is an essential factor for AO7 degradation.

Furthermore, the degradation of AO7 was increased with the decreasing initial pH level. Higher dosage of Cu(II) could promote AO7 degradation, but exceeding the optimal dosage of Cu(II) would quench ·OH and inhibit AO7 degradation. The power of UV light also had a strong

Table 2 | The products of AO7 at 5 min in the Cu(II)/O_2/UV process

Products	p-benzoquinone	2-(3-hydroxypropyl) phenol	3,4-dihydronaphthalene-1(2H)	3-(2-aminophenyl)propanoic acid
Structural formula	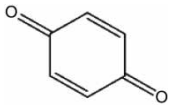	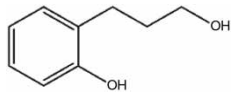	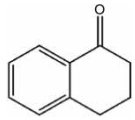	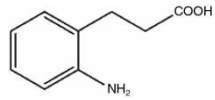
Molecular formula	$C_6H_4O_2$	$C_9H_{12}O_2$	$C_{10}H_{10}O$	$C_9H_{11}O_2N$

Experimental conditions: $[Cu(II)]_0 = 10\ \mu M$, $[AO7]_0 = 1.5\ \mu M$, power of UV light = 15 W, O_2 flow rate = 0.5 L·min^{-1}, pH = 3.5 ± 0.1, 20 °C.

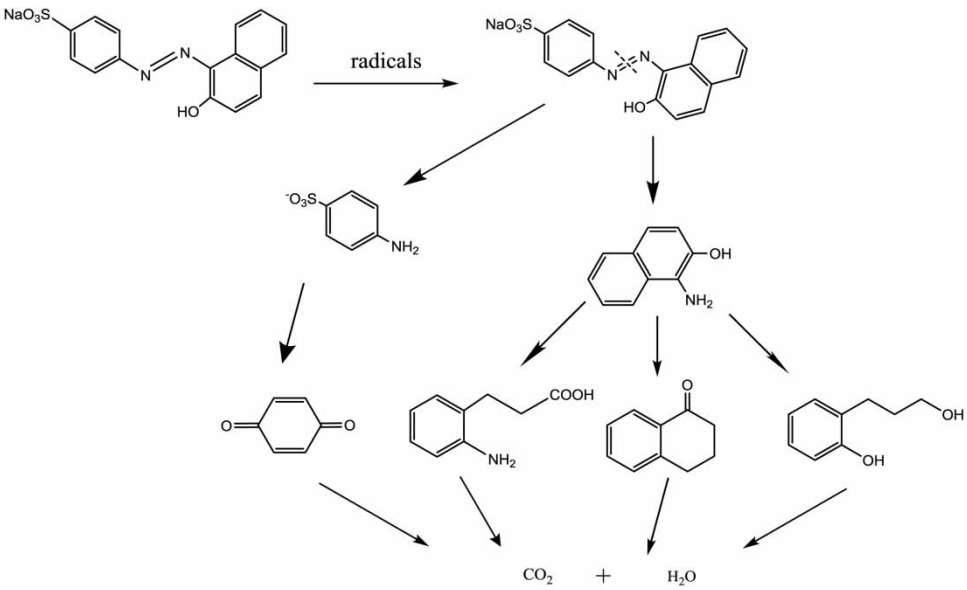

Figure 13 | The degradation process of AO7 in the Cu(II)/O_2/UV process.

effect on the degradation of AO7, and the higher power of UV light enhanced the degradation of AO7. The AO7 degradation followed the pseudo-first order kinetics, indicating that an increased dosage of AO7 inhibited the degradation of AO7. AO7 was further oxidized to CO_2 and H_2O in the Cu(II)/O_2/UV process.

ACKNOWLEDGEMENTS

Appreciation and acknowledgments are given to the National Natural Science Foundation of China (No. 51508353), and the National Natural Science Foundation of China (No. 51008052).

REFERENCES

Ahmed, B., Limem, E., Abdel-Wahab, A. & Nasr, B. 2011 Photo-Fenton treatment of actual agro-industrial wastewaters. *Ind. Eng. Chem. Res.* **50** (11), 6673–6680.

Anipsitakis, G. P. & Dionysiou, D. D. 2004 Radical generation by the interaction of transition metals with common oxidants. *Environ. Sci. Technol.* **38** (13), 3705–3712.

APHA/AWWA/WEF 2005 *Standard Methods for the Examination of Water & Wastewater*, 21st edn. American Public Health Association/American Water Works Association/Water Environment Federation, Washington, DC, USA.

Babel, S., Sekartaji, P. A. & Sudrajat, H. 2017 TiO_2 as an effective nanocatalyst for photocatalytic degradation of humic acid in water environment. *J. Water Supply Res. Technol. AQUA* **66** (1), 25–35.

Bader, H., Sturzenegger, V. & Hoigne, J. 1988 Photometric method for the determination of low concentrations of hydrogen

peroxide by the peroxidase catalyzed oxidation of N,N-diethyl-p-phenylenediamine (DPD). *Water Res.* **22** (9), 1109–1115.

Bauer, C., Jacques, P. & Kalt, A. 2001 Photooxidation of an azo dye induced by visible light incident on the surface of TiO_2. *J. Photochem. Photobiol. A Chem.* **140** (1), 87–92.

Behnajady, M. A., Modirshahla, N. & Shokri, M. 2004 Photodestruction of Acid Orange 7 (AO7) in aqueous solutions by UV/H_2O_2: influence of operational parameters. *Chemosphere* **55** (1), 129–134.

Bokare, A. D. & Choi, W. Y. 2015 Singlet-oxygen generation in alkaline periodate solution. *Environ. Sci. Technol.* **49**, 14392–14400.

Buxton, G. V., Greenstock, C. L., Helman, W. P. & Ross, A. B. 1988 Critical review of rate constants for reactions of hydrated electrons chemical kinetic data base for combustion chemistry, hydrogen atoms and hydroxyl radicals (·OH/·O^-) in aqueous solution. *J. Phys. Chem. Ref. Data* **17** (2), 513–886.

Chen, L. W., Ma, J., Li, X. C., Zhang, J., Fang, J. Y., Guan, Y. H. & Xie, P. C. 2011 Strong enhancement on Fenton oxidation by addition of hydroxylamine to accelerate the ferric and ferrous iron cycles. *Environ. Sci. Technol.* **45** (9), 3925–3930.

Devi, L. G., Munikrishnappa, C., Nagaraj, B. & Rajashekhar, K. E. 2013 Effect of chloride and sulfate ions on the advanced photo Fenton and modified photo Fenton degradation process of Alizarin Red S. *J. Mol. Catal. A Chem.* **374–375**, 125–131.

Jun, Z., Wu, D. & Lown, J. W. 1992 Photosensitization by anticancer agents 12 Perylene quinonoid pigments, a novel type of singlet oxygen sensitizer. *J. Photochem. Photobiol. A Chem.* **64**, 273–287.

Kang, D. E., Lim, C. H., Kim, J. Y., Kim, E. S., Chun, H. J. & Cho, B. R. 2014 Two-photon probe for Cu^{2+} with an internal reference: quantitative estimation of Cu^{2+} in human tissues by two-photon microscopy. *Anal. Chem.* **86** (11), 5353–5359.

Keenan, C. R. & Sedlak, D. L. 2008 Factors affecting the yield of oxidants from the reaction of nanoparticulate zero-valent iron and oxygen. *Environ. Sci. Technol.* **42** (4), 1262–1267.

Kolthoff, I. M. & Woods, R. 1966 Polarographic kinetic currents in mixtures of persulfate and copper(II) in chloride medium. *J. Am. Chem. Soc.* **7** (88), 1371–1375.

Lam, S. W., Hermawan, M., Coleman, H. M., Fisher, K. & Amal, R. 2007 The role of copper(II) ions in the photocatalytic oxidation of 1,4-dioxane. *J. Mol. Catal. A Chem.* **278**, 152–159.

Lee, H., Lee, H. J., Seo, J., Kim, H. E., Shin, Y. K., Kim, J. H. & Lee, C. 2016 Activation of oxygen and hydrogen peroxide by copper(II) coupled with hydroxylamine for oxidation of organic contaminants. *Environ. Sci. Technol.* **50** (15), 8231–8238.

Li, X. N., Liu, J. Y., Rykov, A. I., Han, H. X., Jin, C. Z., Liu, X. & Wang, J. H. 2015 Excellent photo-Fenton catalysts of Fe-Co Prussian blue analogues and their reaction mechanism study. *Appl. Catal. B Environ.* **175**, 196–205.

Liang, C. J. & Su, H. W. 2009 Identification of sulfate and hydroxyl radicals in thermally activated persulfate. *Ind. Eng. Chem. Res.* **11** (48), 5558–5562.

Liu, R., Goodell, B., Jellison, J. & Amirbahman, A. 2005 Electrochemical study of 2,3-dihydroxybenzoic acid and its interaction with Cu(II) and H_2O_2 in aqueous solutions: implications for wood decay. *Environ. Sci. Technol.* **39** (1), 175–180.

Liu, W. P., Zhang, H. H., Cao, B. P., Lin, K. D. & Gan, J. 2011 Oxidative removal of bisphenol A using zero valent aluminum–acid system. *Water Res.* **45** (4), 1872–1878.

Ma, J. & Graham, N. J. D. 2000 Degradation of atrazine by manganese-catalysed ozonation-influence of radical scavengers. *Water Res.* **34** (15), 3822–3828.

Noradoun, C. E. & Cheng, I. F. 2005 EDTA degradation induced by oxygen activation in a zerovalent iron/air/water system. *Environ. Sci. Technol.* **39** (18), 7158–7163.

Norzaee, S., Djahed, B., Khaksefidi, R. & Mostafapour, F. K. 2017 Photocatalytic degradation of aniline in water using CuO nanoparticles. *J. Water Supply Res. Technol. AQUA* **66** (3), 178–185.

Pham, A. N., Rose, A. L. & Waite, T. D. 2012 Kinetics of Cu(II) reduction by natural organic matter. *J. Phys. Chem. A* **116** (25), 6590–6599.

Qi, C. D., Liu, X. T., Ma, J., Lin, C. Y., Li, X. W. & Zhang, H. J. 2016 Activation of peroxymonosulfate by base: implications for the degradation of organic pollutants. *Chemosphere* **151**, 280–288.

Qin, Y. X., Song, F. H., Ai, Z. H., Zhang, P. P. & Zhang, L. Z. 2015 Protocatechuic acid promoted alachlor degradation in Fe(III)/H_2O_2 Fenton system. *Environ. Sci. Technol.* **49** (13), 7948–7956.

Rosenfeldt, E. J., Melcher, B. & Linden, K. G. 2005 UV and UV/H_2O_2 treatment of methylisoborneol (MIB) and geosmin in water. *J. Water Supply Res. Technol. AQUA* **54** (7), 423–434.

Son, Y., Lim, M., Khim, J. & Ashokkumar, M. 2012 Attenuation of UV light in large-scale sonophotocatalytic reactors: the effects of ultrasound irradiation and TiO_2 concentration. *Ind. Eng. Chem. Res.* **51** (1), 232–239.

Thomas, C., Wu, M. & Billingsley, K. L. 2016 Amination–oxidation strategy for the copper-catalyzed synthesis of monoarylamines. *J. Org. Chem.* **81** (1), 330–335.

Waldemer, R. H., Tratnyek, P. G., Johnson, R. L. & Nurmi, J. T. 2007 Oxidation of chlorinated ethenes by heat-activated persulfate: kinetics and products. *Environ. Sci. Technol.* **41** (3), 1010–1015.

Wang, J. L., Wang, C. & Lin, W. B. 2012 Metal–organic frameworks for light harvesting and photocatalysis. *ACS Catal.* **2** (12), 2630–2640.

Wang, D. B., Zhao, L. X., Guo, L. H. & Zhang, H. 2014 Online detection of reactive oxygen species in ultraviolet (UV)-irradiated nano-TiO_2 suspensions by continuous flow chemiluminescence. *Anal. Chem.* **86** (21), 10535–10539.

Wasserman, H. H., Scheffer, J. R. & Cooper, J. L. 1972 Singlet oxygen reactions with 9,10-diphenylanthracene peroxide. *J. Am. Chem. Soc.* **14** (94), 4991–4996.

Wen, G., Wang, S. J., Ma, J., Huang, T. L., Liu, Z. Q., Zhao, L. & Xu, J. L. 2014 Oxidative degradation of organic pollutants in aqueous solution using zero valent copper under aerobic atmosphere condition. *J. Hazard. Mater.* **275**, 193–199.

Wu, K. Q., Xie, Y. D., Zhao, J. C. & Hidaka, H. 1999 Photo-Fenton degradation of a dye under visible light irradiation. *J. Mol. Catal. A Chem.* **144**, 77–84.

Wu, F., Deng, N. S. & Hua, H. L. 2000 Degradation mechanism of azo dye C. I. reactive red 2 by iron powder reduction and photooxidation in aqueous solutions. *Chemosphere* **41** (8), 1233–1238.

Wu, C., Shemer, H. & Linden, K. G. 2007 Photodegradation of metolachlor applying UV and UV/H_2O_2. *J. Agric. Food Chem.* **55** (10), 4059–4065.

Xu, Z., Shan, C., Xie, B. H., Liu, Y. & Pan, B. C. 2017 Decomplexation of Cu(II)-EDTA by UV/persulfate and UV/H_2O_2: efficiency and mechanism. *Appl. Catal. B Environ.* **200**, 439–447.

Yao, H., Sun, P. Z., Minakata, D., Crittenden, J. C. & Huang, C. H. 2013 Kinetics and modeling of degradation of ionophore antibiotics by UV and UV/H_2O_2. *Environ. Sci. Technol.* **47** (9), 4581–4589.

Yuan, X., Pham, A. N., Xing, G. W., Rose, A. L. & Waite, T. D. 2012 Effects of pH, chloride, and bicarbonate on Cu(I) oxidation kinetics at circumneutral pH. *Environ. Sci. Technol.* **46** (3), 1527–1535.

Yuan, X., Pham, A. N., Miller, C. J. & Waite, T. D. 2013 Copper-catalyzed hydroquinone oxidation and associated redox cycling of copper under conditions typical of natural saline waters. *Environ. Sci. Technol.* **47** (15), 8355–8364.

Zeng, Z. Q., Zou, H. K., Li, X., Sun, B. C., Chen, J. F. & Shao, L. 2012 Ozonation of phenol with O_3/Fe(II) in acidic environment in a rotating packed bed. *Ind. Eng. Chem. Res.* **51** (31), 10509–10516.

Zhang, H. H., Cao, B. P., Liu, W. P., Lin, K. D. & Feng, J. 2012 Oxidative removal of acetaminophen using zero valent aluminum-acid system: efficacy, influencing factors, and reaction mechanism. *J. Environ. Sci.* **24** (2), 314–319.

Zhao, Q. & Zhang, H. Y. 2005 Singlet-oxygen-generating activity of deuterated perylenequinonoid pigments. *Dyes Pigments* **66**, 15–17.

Zhong, Y. H., Liang, X. L., Tan, W., Zhong, Y., He, H. P., Zhu, J. X., Yuan, P. & Jiang, Z. 2013 A comparative study about the effects of isomorphous substitution of transition metals (Ti, Cr, Mn, Co and Ni) on the UV/Fenton catalytic activity of magnetite. *J. Mol. Catal. A Chem.* **372**, 29–34.

Zhou, P., Zhang, J., Liang, J., Zhang, Y. L., Liu, Y. & Liu, B. 2016 Activation of persulfate/copper by hydroxylamine via accelerating the cupric/cuprous redox couple. *Water Sci. Technol.* **3** (73), 493–500.

Zou, J. P., Wu, D. D., Luo, J. M., Xing, Q. J., Luo, X. B., Dong, W. H., Luo, S. L., Du, H. M. & Suib, S. L. 2016 A strategy for one-pot conversion of organic pollutants into useful hydrocarbons through coupling photodegradation of MB with photoreduction of CO_2. *ACS Catal.* **6**, 6861–6867.

First received 9 March 2017; accepted in revised form 16 July 2017. Available online 8 September 2017